Supplementary Materials:

This document includes additional figures that are referenced in the manuscript to avoid excessive length in the main paper. Figures S1 to S6 depict the results of the analysis conducted on the remaining stations within the X5 network, focusing on back-azimuthal section plots and H-k stacking. Figure S7 illustrates the impact of deconvolution techniques on the outcomes generated by DeepRFQC, while Figure S8 demonstrates the application of the SNR method to waveforms obtained from St. John's station (SJNN). Additionally, Table S1 provides a comprehensive comparison between manual and automated quality control procedures, alongside a comparison with findings reported by Thompson et al., 2010.

To assess the global applicability of this algorithm, we tested DeepRFQC on a 6-year dataset from the ANTO station in Ankara, Turkey. In this evaluation, we compared the data processed using the same preprocessing techniques as in this study with data processed using different methods, including bandpass filters between 0.05 and 1 Hz and multitaper deconvolution (Figure S9). Although applying water-level filtering with a bandpass between 0.05 and 0.5 Hz yielded better results, the alternative settings provided valuable and informative insights, even in regions geographically far distant from the original study area.

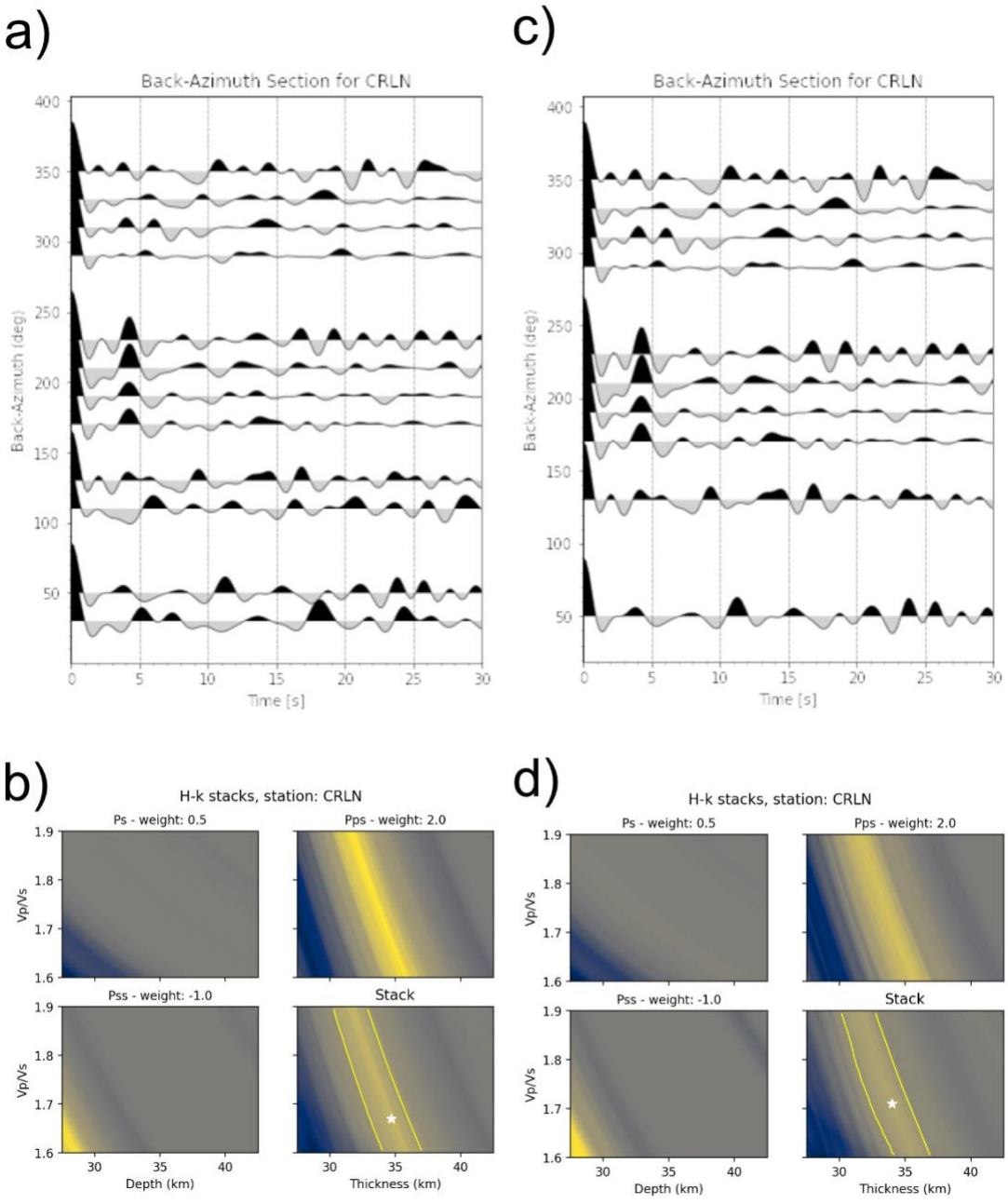

Figure S1. Results of the analysis for station CRLN, a, and c) back-azimuth section plots for manual and automated QC, respectively, b and d) H-κ stacking for manual and automated QC, respectively.

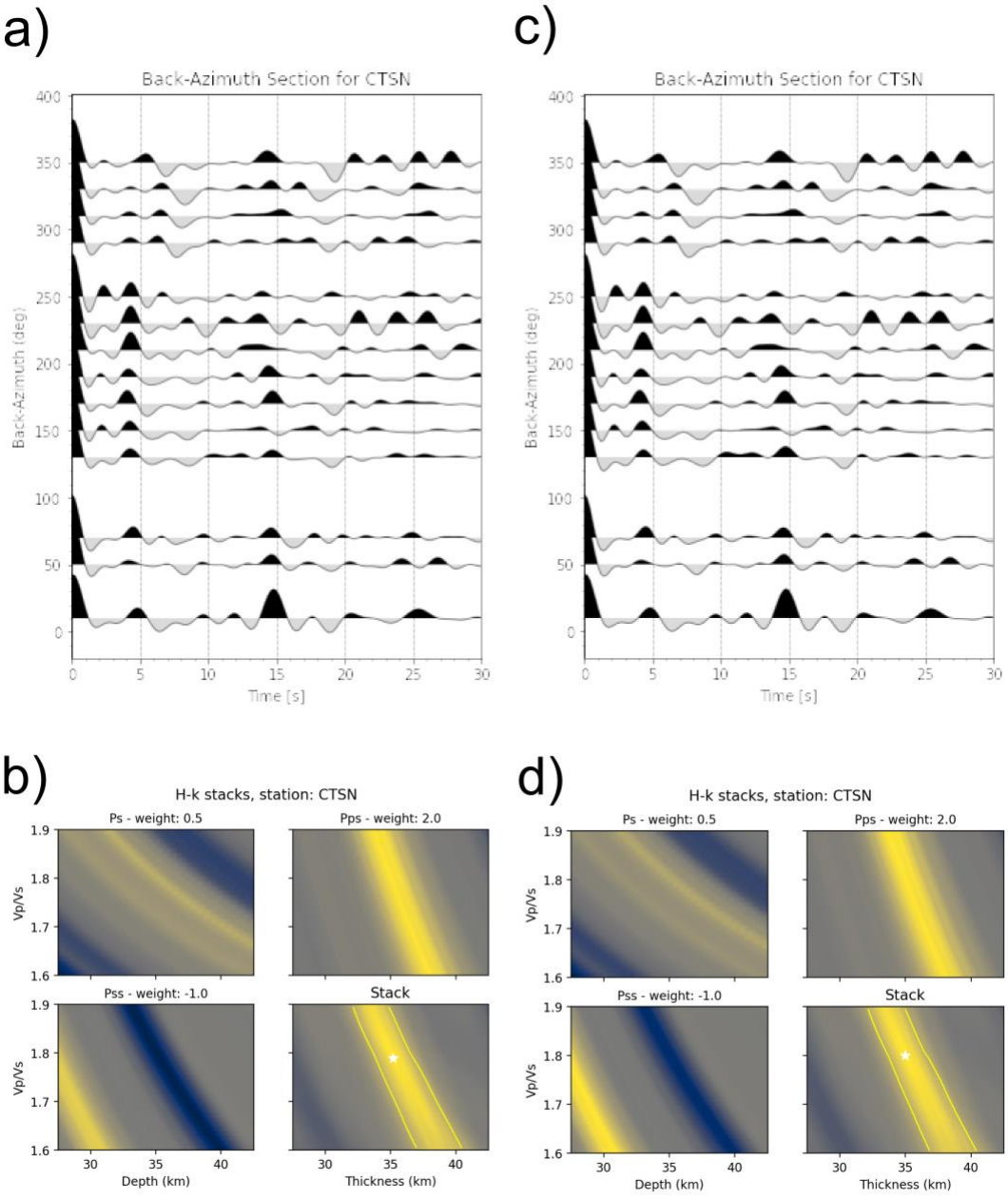

Figure S2. Results of the analysis for station CTSN, a, and c) back-azimuth section plots for manual and automated QC, respectively, b and d) H-κ stacking for manual and automated QC, respectively.

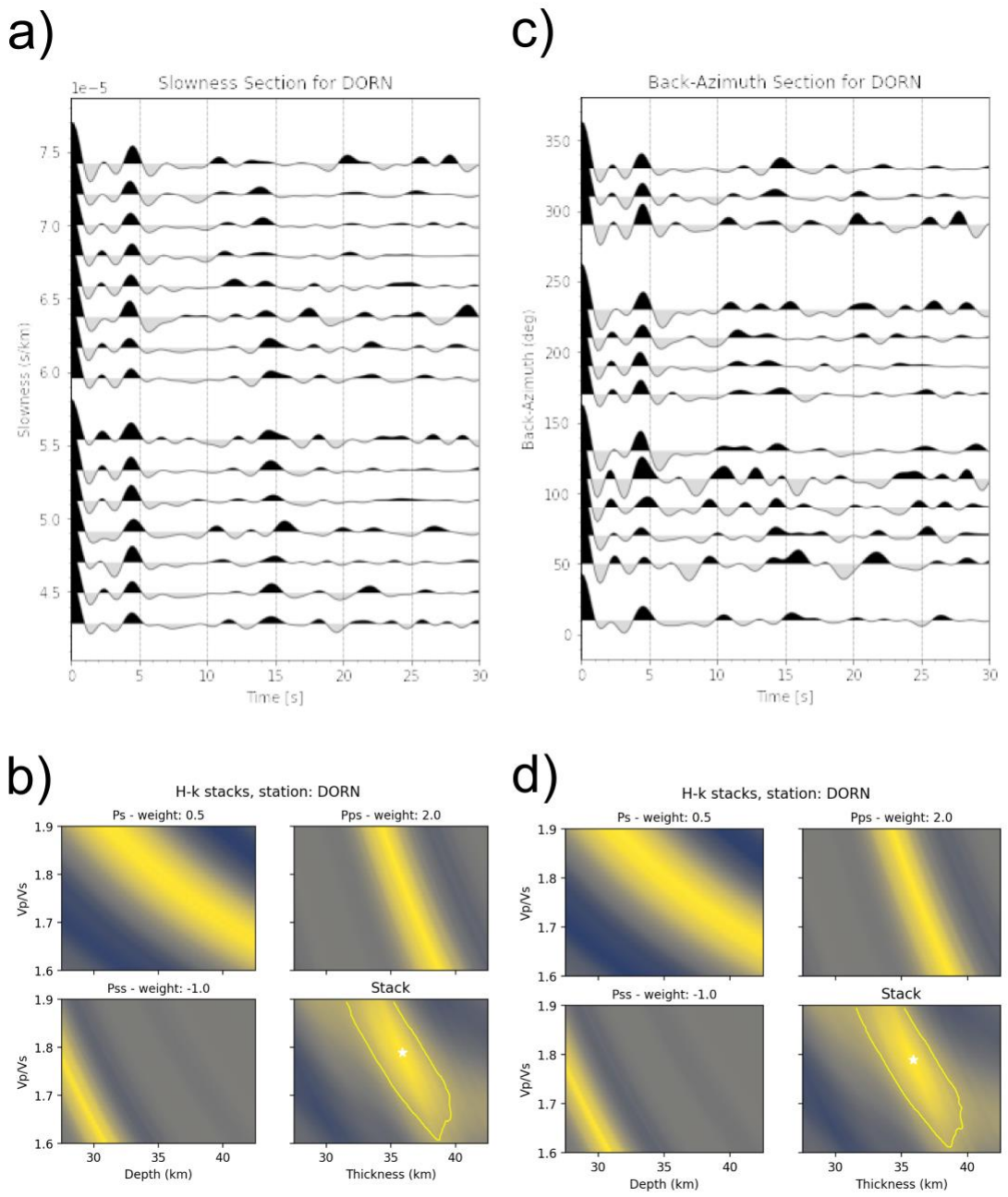

Figure S3. Results of the analysis for station DORN, a, and c) back-azimuth section plots for manual and automated QC, respectively, b and d) H-κ stacking for manual and automated QC, respectively.

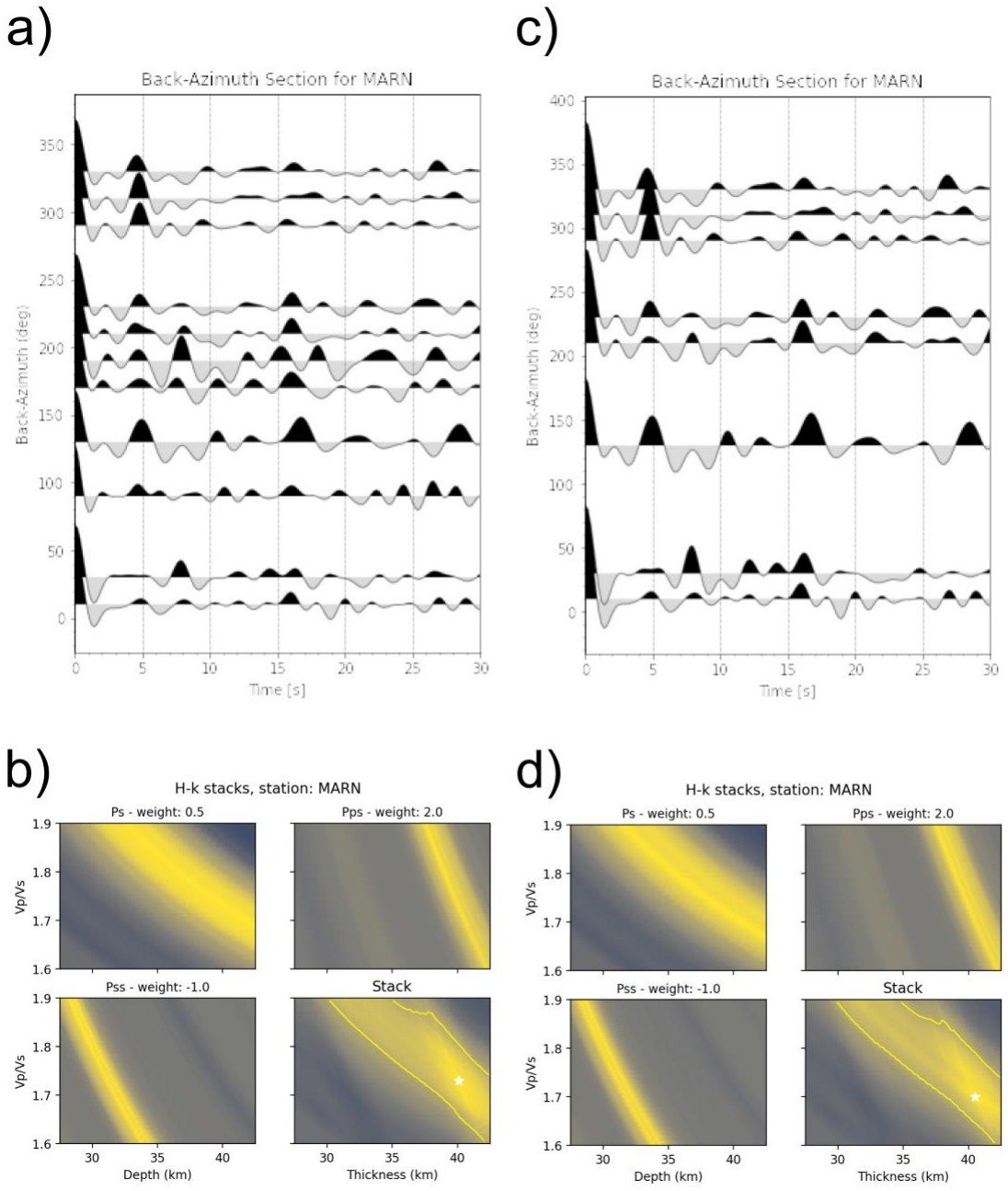

Figure S4. Results of the analysis for station MARN, a, and c) back-azimuth section plots for manual and automated QC, respectively, b and d) H-κ stacking for manual and automated QC, respectively.

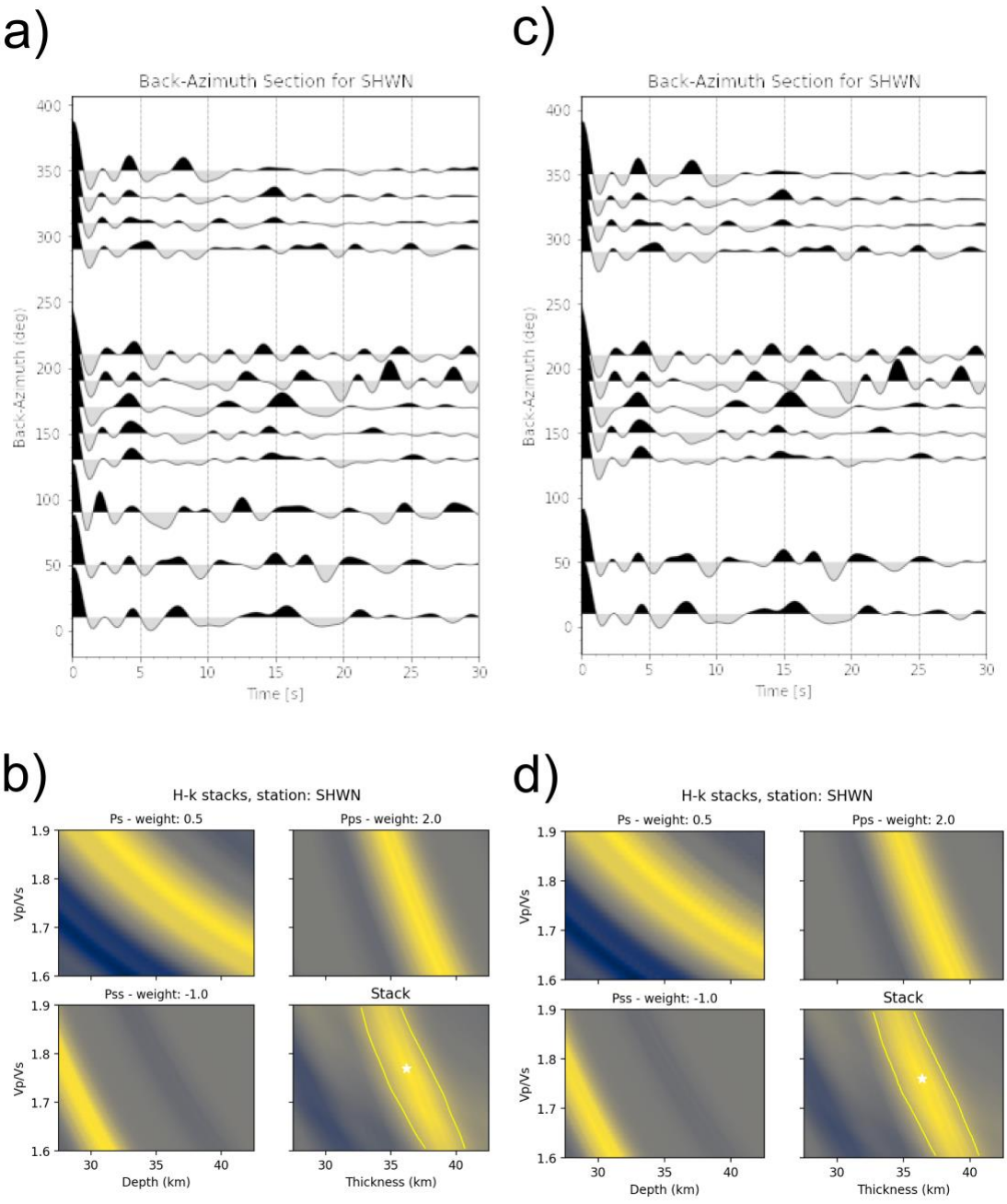

Figure S5. Results of the analysis for station SHWN, a, and c) back-azimuth section plots for manual and automated QC, respectively, b and d) H-κ stacking for manual and automated QC, respectively.

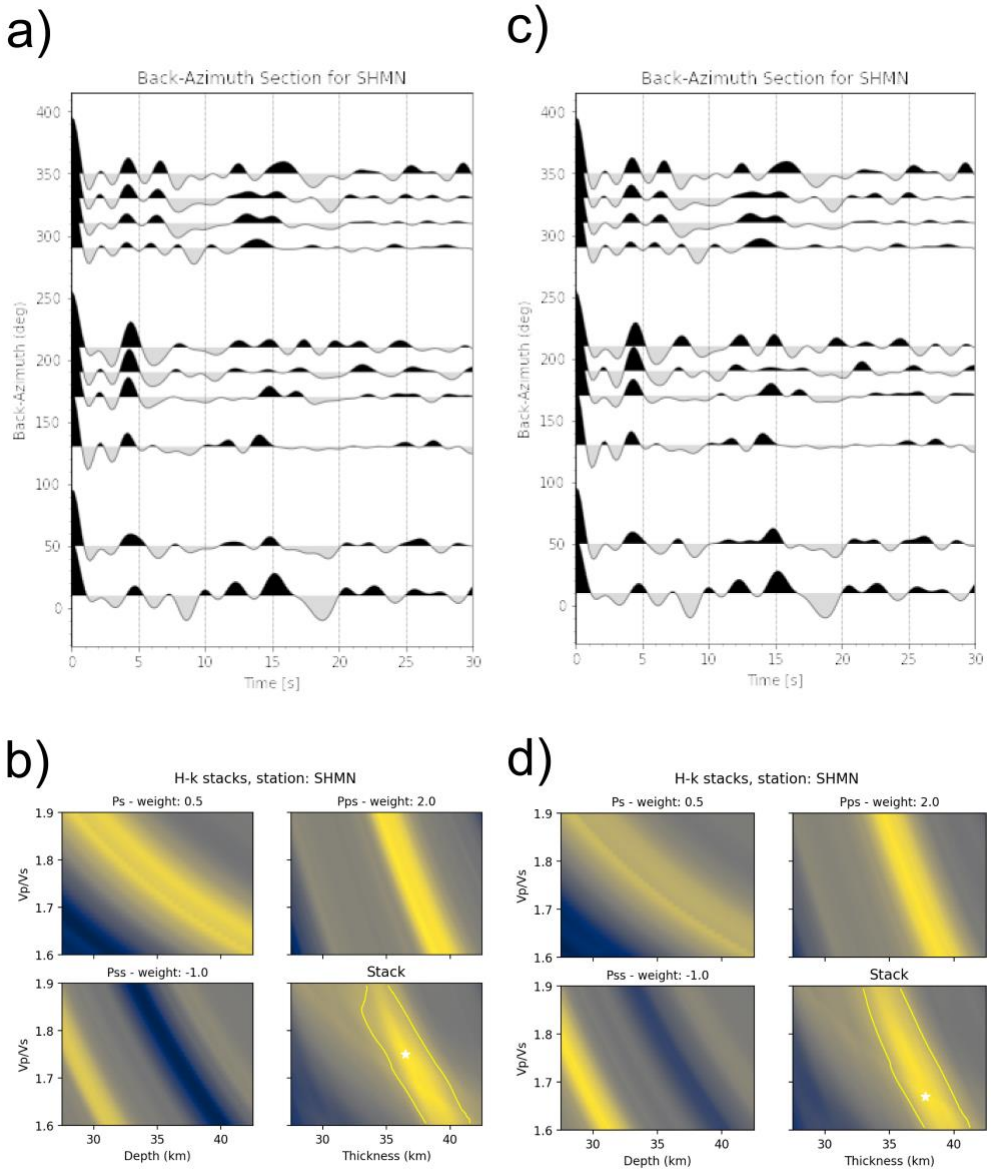

Figure S6. Results of the analysis for station SHMN, a, and c) back-azimuth section plots for manual and automated QC, respectively, b and d) H-κ stacking for manual and automated QC, respectively.

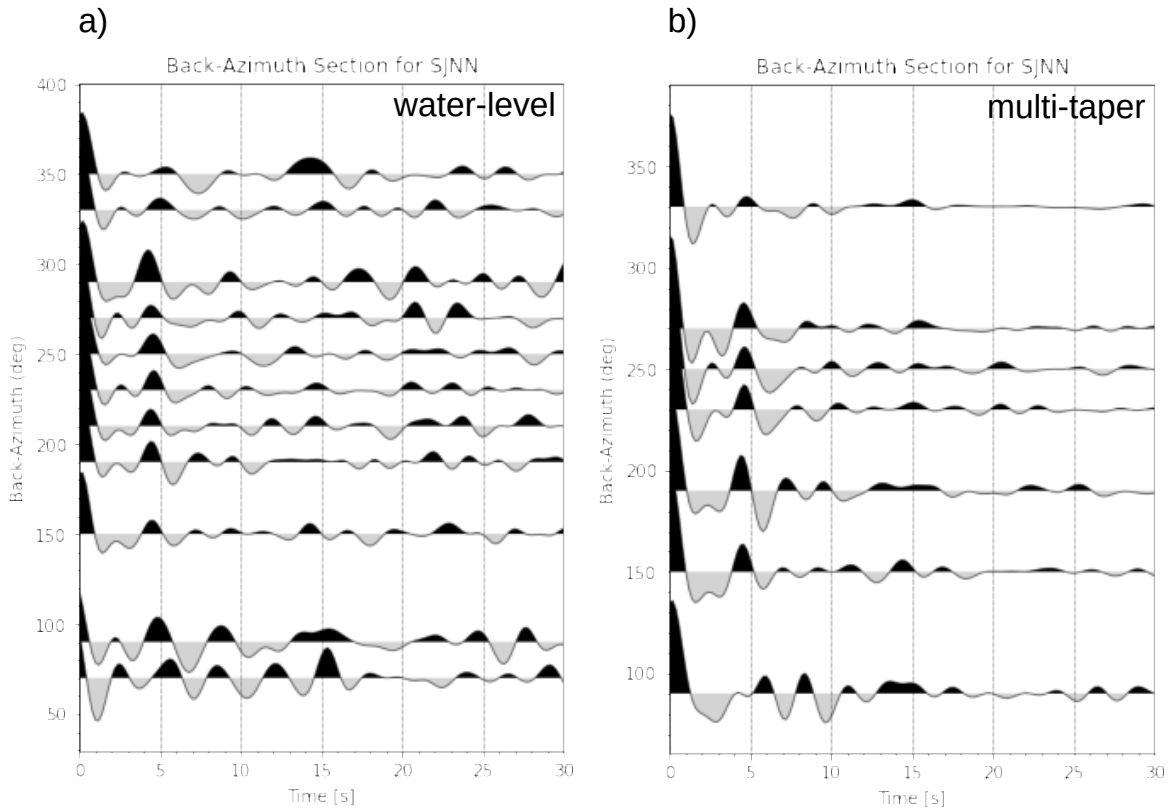

Figure S7. Comparison of the effect of deconvolution techniques on the results for station SJNN (St. Johns, NL, CA) by DeepRFQC, using a) water-level and b) multi-taper methods.

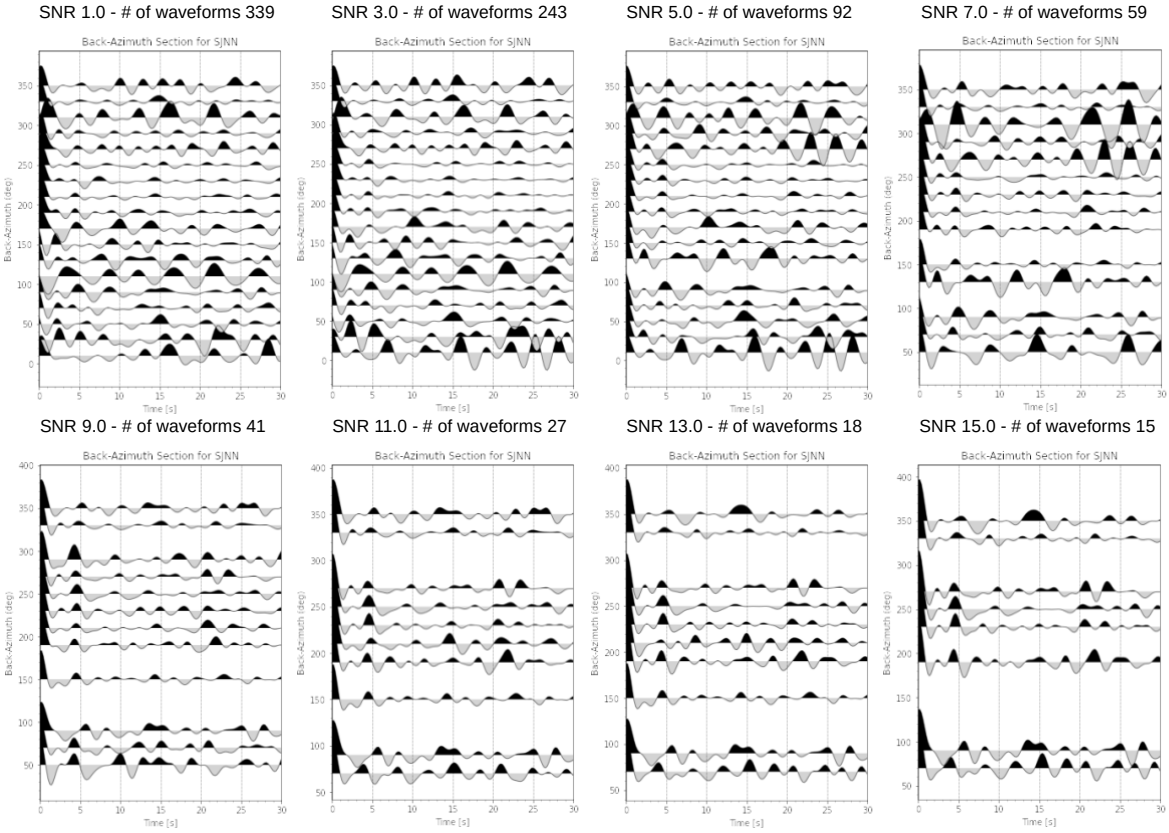

Figure S8. Results of SNR quality control for station SJNN (St. Johns, NL, CA) using different levels of SNR threshold from 1 to 15.

Station	Manual					Automated					Thompson et al. (2010)	
	H	H error	k	k error	# stacks	H	H error	k	k error	# stack	H	k
CRLN	34.0	1.67	1.71	0.07	39	34.7	1.67	1.67	0.07	40	36.0	1.73
CTSN	35.2	2.07	1.79	0.07	50	35.0	2.05	1.80	0.07	48	36.6	1.75
MANN	33.6	2.07	1.83	0.07	43	33.2	2.17	1.85	0.07	37	35.4	1.74
MARN	40.1	3.07	1.73	0.07	49	40.5	3.15	1.70	0.070	41	N/A	N/A
DORN	35.9	2.00	1.79	0.07	83	35.9	2.0	1.79	0.07	80	36.6	1.77
NOTN	35.8	2.45	1.74	0.07	45	35.6	2.17	1.74	0.07	43	36.3	1.75
SHWN	36.2	1.97	1.77	0.08	40	36.4	2.0	1.76	0.07	39	38.0	1.70
SHMN	36.5	2.12	1.75	0.07	42	37.8	2.07	1.67	0.07	30	37.2	1.73

Table S1. Comparison of H-κ analysis using manual and automated quality control methods and a comparison with results obtained by Thompson et al. (2010) all with v_p equals to 6.5 km/s.

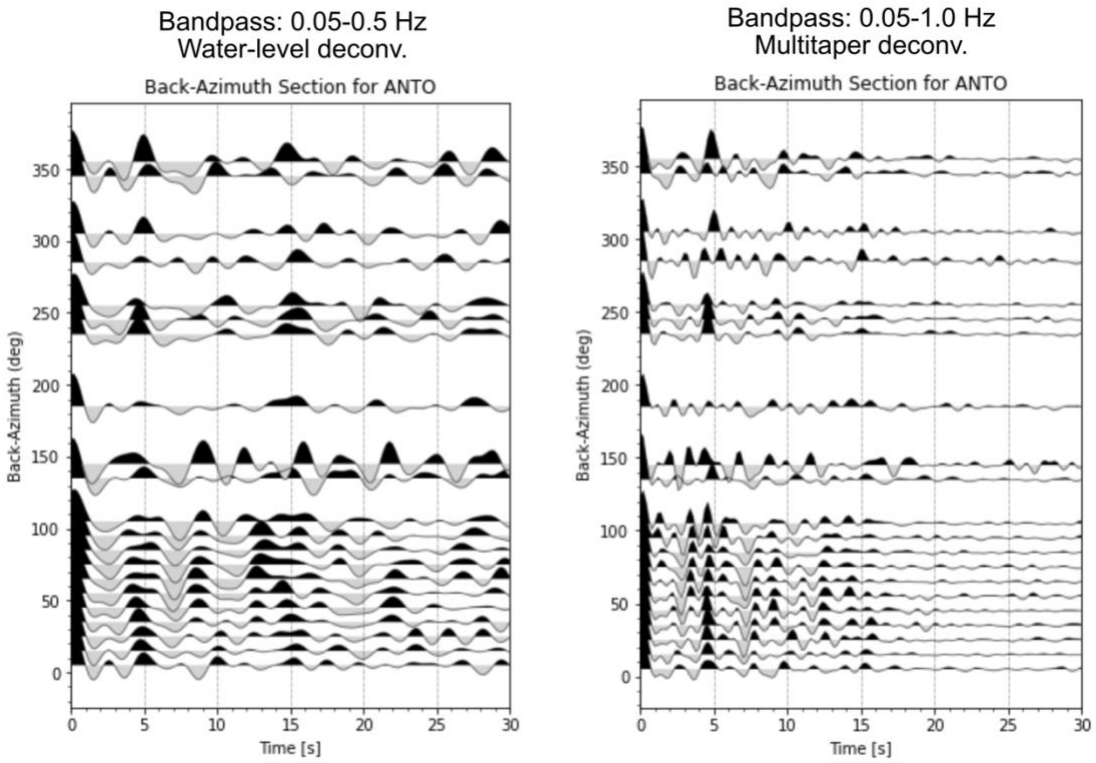

Figure S9. Results of applying DeepRFQC to data from the station ANTO, Ankara, Turkey, for two different deconvolution methods: a) bandpass filter between 0.05 and 0.5 Hz and water level deconvolution, b) bandpass filter between 0.05 and 1.0 Hz and multitaper deconvolution.